Exploring the anti-EBV potential of suberoylanilide hydroxamic acid: induction of apoptosis in infected cells through suppressing BART gene expression and inducing lytic infection

Yuxin Liu[1], Aung Phyo Wai[1], Tumurgan Zolzaya[1], Yuichi Iida[2], Shunpei Okada[1], Hisashi Iizasa[1] *, and Hironori Yoshiyama[1] *

[1]*Department of Microbiology, Faculty of Medicine, Shimane University, 89-1 Enya, Izumo, Shimane 693-8501, Japan*

[2] *Department of Immunology, Faculty of Medicine, Shimane University, 89-1 Enya, Izumo, Shimane 693-8501, Japan*

* Corresponding authors

E-mail addresses: m209431@med.shimane-u.ac.jp (Y. Liu), aungpwai@med.shimane-u.ac.jp (A. P. Wai), aungpwai@med.shimane-u.ac.jp (T. Zolzaya), s.okada@med.shimane-u.ac.jp (S. Okada), iizasah@med.shimane-u.ac.jp (H. Iizasa), yosiyama@med.shimane-u.ac.jp (H. Yoshiyama)

Keywords: Epstein–Barr virus; BART microRNA; histone deacetylase inhibitor; tumor lysis; EBV-associated gastric cancer

ABSTRACT

Epstein-Barr virus (EBV) is linked to lymphoma and epithelioma but lacks drugs specifically targeting EBV-positive tumors. *Bam*HI A Rightward Transcript (BART) miRNAs are expressed in all EBV-positive tumors, suppressing both lytic infection and host cell apoptosis. We identified suberoylanilide hydroxamic acid (SAHA), an inhibitor of histone deacetylase enzymes, as an agent that suppresses BART promoter activity and transcription of BART miRNAs. SAHA treatment demonstrated a more pronounced inhibition of cell proliferation in EBV-positive cells compared to EBV-negative cells, affecting both p53 wild-type and mutant gastric epithelial cells. SAHA treatment enhanced lytic infection in wild-type EBV-infected cells, while also enhancing cell death in BZLF1-deficient EBV-infected cells. It reduced BART gene expression by 85% and increased the expression of proapoptotic factors targeted by BART miRNAs. These findings suggest that SAHA not only induces lytic infection but also leads to cell death by suppressing BART miRNA transcription and promoting the apoptotic program.

Highlights

The Epstein-Barr virus (EBV) gives rise to tumors from latently infected cells. Among the approximately 10 latent EBV genes, BART miRNAs are consistently expressed regardless of the type of latency. BART miRNAs constitute a cluster of 40 miRNAs located in the BamHI-A

rightward transcripts (BART) region of the genome. These BART miRNAs are known to play roles in cell proliferation, differentiation, apoptosis induction, immune evasion, and so on. Our research focused on the BART promoter, which commonly controls the expression of every BART miRNA. We discovered that SAHA can inhibit BART promoter activity. Treatment of EBV-positive gastric epithelial cells with SAHA led to both lytic infection and apoptotic cell death. Interestingly, even in cells infected with EBV lacking the BZLF1 gene, which doesn't induce lytic infection, SAHA treatment induced cell death in virus-infected cells. Therefore, by targeting the expression of BART miRNAs, we might develop novel drugs to combat EBV infection.

1. Introduction

Epstein–Barr virus (EBV) is a ubiquitous gamma herpes virus with two life cycles: a lytic infection with rapid replication of the viral genome, and a latent infection where only a limited number of viral genes are expressed, causing an increase in the number of viral genomes in line with the amount of cell division (Murata et al., 2021). While many infected individuals remain asymptomatic throughout their lives, some show a severe acute infection (called infectious mononucleosis) and others may develop lymphoma or epithelial tumors due to continuous EBV infection (Young et al., 2016, Münz, 2019).

In EBV-associated cancers, specific viral latent genes play multiple roles in tumor formation. Among these genes, EBV nuclear antigen 1 (EBNA1) is consistently expressed in all tumor cells. Additionally, EBV-encoded small RNA (EBER) and *BamH*I A rightward transcript (BART), which are not translated into proteins, are also expressed (iizasa et al., 2012, Marquitz, 2015). In particular, significant attention has been directed towards the 40 microRNAs (miRNAs) encoded within the intron of the BART gene. These miRNAs are noteworthy due to their ability to suppress apoptosis, immune reactions, and lytic infections, potentially contributing to tumor formation and maintenance (Cai et al., 2006, Klinke et al., 2014, iizasa et al., 2020, De Re et al., 2020). Specifically, BART miRNA expression is higher in epithelial tumors compared to B lymphomas (Qiu et al., 2011, Yang et al., 2013).

BART miRNAs play a role in the development of EBV-related epithelial cancers through targeting apoptosis-inducing factors such as castor zinc finger 1a (CASZ1a), octamer-binding transcription factor 1 (OCT1), tumor protein p53-inducible nuclear protein 1 (TP53INP1), and AT-rich interaction domain 2 (ARID2) (Kang et al., 2015). These BART miRNAs suppress apoptosis through affecting multiple pathways. In addition, we have observed that miR-BART22-3p reduces the expression of N-myc downstream-regulated gene 1 (NDRG1), contributing to the malignant phenotype of nasopharyngeal carcinomas (Kanda et al., 2015). It has been demonstrated that not only miR-BART22-3p but also multiple other BART miRNAs

target NDRG1(Kanda et al., 2015). Considering that several BART miRNAs often converge on a single gene, it is implied that suppressing the entire transcription of the BART gene may be a more effective strategy to exert potent anti-tumor activity (Iizasa et al., 2020).

BART miRNA expression is regulated by two promoters, P1 and P2 (De Jesus et al., 2003, Chen et al., 2005), with reduced DNA methylation observed in epithelial cells compared to B cells (Kim et al., 2011). Consequently, these promoters are more active in epithelial cells, resulting in increased miRNA expression. Monitoring the transcriptional activity of the BART promoter facilitates the screening of inhibitors for BART miRNA transcription. Through a luciferase assay system, we have identified several potential drugs among 1,200 FDA-approved compounds that may effectively inhibit BART promoter transcription.

Suberoylanilide hydroxamic acid (SAHA, Vorinostat) is a histone deacetylase (HDAC) inhibitor used to treat cutaneous T-cell lymphoma. A previous study has suggested that SAHA enhances the expression of the EBV immediate-early gene *Bam*HI Z fragment leftward open reading frame 1 (BZLF1), which triggers lytic infection (Countryman et al., 1985, Hui et al., 2010, Daigle et al., 2011). During lytic infection, massive EBV replication induces apoptosis in infected cells (Murata et al., 2021, Kawanishi et al., 1993). Consequently, agents stimulating lytic EBV infection hold promise as targeted therapeutic drugs for EBV-associated cancers. However, in EBV-associated cancer cells, viral genomes sometimes become deficient as the

host cell progresses in malignancy (Okuno et al., 2019). Tumor cells carrying defective viruses that lack the ability to switch from latent to lytic infection may not respond to tumor lysis therapy. Therefore, drugs that selectively target and harm EBV-infected cells should not induce lytic infection.

In our study, SAHA was identified as a drug capable of suppressing the activity of the BART gene promoter. Intriguingly, SAHA was observed to selectively enhance cell death in EBV-positive cells, both in the presence and absence of lytic infection induction.

2. Materials and Methods

2.1. Cell culture and Virus

The AGS cells with wild-type p53, which originated from a human gastric cancer, were purchased from the American Type Culture Collection (Manassas, VA). The MKN28 cells with mutated p53 were obtained from the National Institute of Biomedical Innovation, Health and Nutrition, JCRB Cell Bank (Matozaki et al., 1992) (**Supplementary 1**). Recombinant Epstein–Barr virus carrying enhanced green fluorescent protein (eGFP) and a neomycin resistance gene inserted into the BXLF1 thymidine kinase gene region of the virus (eGFP-EBV) was used to infect each cell line. The infectivity and proliferative capacity of eGFP-EBV were comparable to the parental Akata EBV strain (Maruo et al., 2001). AGS BZLF1-KO EBV cells were established

through infecting AGS cells with a virus produced by introducing the BZLF1 gene into Akata cells persistently infected with BZLF1-KO EBV (Katsumura et al., 2009).

These cells were cultured in RPMI-1640 medium (Sigma-Aldrich, St. Louis, MO) supplemented with 10% fetal bovine serum (FBS, ThermoFisher Scientific, Waltham, MA), 100 units/mL of penicillin and 100 μg/mL of streptomycin (Nacalai, Kyoto, Japan) at 37 °C in a 5% CO_2 incubator. AGS and MKN28 cells were infected with eGFP-EBV, then selected through culturing in medium containing 420 and 560 μg/mL G418 (Promega, Madison, WI), respectively. Persistently EBV-infected AGS EBV cells and MKN28 EBV cells were established.

2.2. Promoter assay

The BART promoter (Kim et al., 2019) was cloned and inserted into pNL1.1 (Promega), which had been digested with *Kpn*I and *Hind*III. The secreted NanoLuc (secNL) gene (hall et al., 2012, Nishitsuji et al., 2018) (provided by Dr. Nishitsiuji at Fujita Medical University) was amplified using KOD One polymerase (TOYOBO, Osaka, Japan) and specific primers (F:5'-GTTGTTCCTCAAGCTTGCCACCCATGGGAGTCAAAGTTTGTTTGCCCTGATCTG-3'; R: 5'-TCGCGTCGACTAAGATACATTGATGAGTTTGGACAAACACAACTAGAATGCA-3'). The pNL1.1 vector was digested with *Hind*III and *Xba*I, and the NanoLuc gene was replaced with the secNL gene using the In-Fusion Snap Assembly Master Mix (Takara Bio, Shiga, Japan).

Moreover, the vector was digested with *Bam*HI and *Sal*I, and the bleomycin resistance gene, which was PCR amplified from pENTR_H1 (ThermoFisher) using specific primers (F: 5'-TCGCGGATCCGTGTGTCAGTTAGGGTGTGGAAAGTCC-3'; R: 5'-TCGCGTCGACTA AGATACATTGATGAGTTTGGACAAACACAACTAGAATGCA-3'), was incorporated.

The created vector was transferred into AGS cells, and stable expression clones were selected using zeocin (ThermoFisher). The AGS cells expressing secNL regulated by the BART promoter were seeded at 6.25×10^3 cells/well in a 96-well plate, and the next day, 0.1% dimethyl sulfoxide (DMSO, Nacalai), 2.5 μM SAHA, dasatinib, rapamycin, topotecan or ganciclovir (Selleck Chemicals, Houston, TX) dissolved in DMSO was added. After 48 hours of drug treatment, the culture supernatants were collected, and the luciferase activity was measured using the NanoGlo Luciferase Assay (Promega) and the GloMax Navigator System (Promega).

2.3. Cell proliferation assay

Cells were seeded at 6.25×10^3 cells/well in a 96-well plate, and the next day, SAHA dissolved in DMSO was added. The DMSO concentration in the culture medium was set at 0.1%. After 48 hours, 10 μL of CCK-8 (Ishiyama et al., 1996) (DOIJNDO, Kumamoto, Japan) was added to 100 μL of culture medium, and the absorbance at 450 nm was measured using a DTX880 (Beckman Coulter, Brea, CA). Cell viability was calculated as 100% of the absorbance of cells

treated with DMSO alone (the control experiment). The 50% inhibitory concentration (IC_{50}) was calculated using Graphpad Prism (ver. 10.0.3) (Graphpad Software, Boston, MA).

2.4. Apoptosis assay

AGS, AGS EBV, and AGS EBV BZLF1-KO cells were seeded at 2.5×10^5 cells/well in 6-well plates and cultured at 37 °C with 5% CO_2. The cells were treated with 2.5 μM SAHA in 0.1% DMSO for 48 hours. Apoptosis was detected using eBioscience the Annexin V Apoptosis Detection Kit APC (ThermoFisher), eBioscience 7-AAD Viability Stainig Solution (ThermoFisher), and a Cytoflex Flow Cytometer (Beckman Coulter) (**Supplementary 2**). Annexin V+/7-aminoactinomycin D (7-AAD)-positive cells were considered to be in early apoptosis, and Annexin V+/7-AAD+ cells were considered to be in late apoptosis (Schmid et al., 1994). The sum of the number of cells in early and late apoptosis was recorded as the total number of apoptotic cells.

2.5. Quantitative polymerase chain reaction (PCR)

Cells were seeded at a density of 1.1×10^6 cells in a 10 cm dish and treated with 2.5 μM SAHA in 0.1% DMSO for 48 hours. Genomic DNA was extracted from these cells using the GeneElute Mammalian Genomic DNA Miniprep Kit (Sigma-Aldrich) according to the

manufacturer's instructions. The specific primers for the BamHI W region of the EBV genome (F: 5'-CCCAACACTCCACCACACC-3'; R: 5'-TCTTAGGAGGCTGTCCGAGG-3'), human glyceraldehyde 3-phosphate dehydrogenase (GAPDH) gene (F: 5'-TGTGCTCCCACTCCTG ATTTC-3'; R: 5'-CCTAGTCCCAGGGCTTTGATT-3') and dual-quenched fluorescent DNA probes (BamHI W: 5'-FAM/CACACACTA/ZEN/CACACACCCACCCGTCTC/IBFQ-3'; GAPDH: 5'-FAM/CGGTCACAA/ZEN/TCTCCACGC/IBFQ-3') were purchased from Integrated DNA Technologies (IDT) (Coralville, IA).

Quantitative PCR (qPCR) was performed using the SsoAdvanced Universal Probe Supermix (Bio-Rad Laboratories, Hercules, CA) and a CFX Connect Real-Time PCR Detection System (Bio-Rad) (Gelmini et al., 1997, Kartika et al., 2020). GAPDH was used as an internal control for normalization.

2.6. Reverse transcription-qPCR (RT-qPCR)

Approximately 1.1×10^6 cells were seeded into a 10 cm dish and treated with either 0.1% DMSO or 2.5 μM SAHA for 48 hours. Following the standard protocol, total RNA was extracted using ISOGEN (Nippon Gene, Tokyo, Japan). A portion of total RNA was used to synthesize complementary DNA (cDNA) using SuperScript III Reverse Transcriptase (ThermoFisher). The remaining portion was used to synthesize cDNA for the detection of mature miRNA using the

Mir-X™ miRNA First-Strand Synthesis kit (Mir-X™ miRNA, TaKaRa) (**Supplementary 2**). Gene expression was measured using the primers indicated below (**Table 1**). The reverse primer for mature miRNAs used the mRQ3' primer included in the Mir-X™ miRNA kit. The U6 primer that was also used was included in the Mir-X™ miRNA kit. PCR products were detected using the SsoAdvanced Universal SYBR Green Supermix (Bio-Rad) and a CFX Connect Real-Time PCR Detection System. The amplification of the target genes was repeated for 40 cycles with a program of 2 minutes at 98 °C, 10 seconds at 95 °C, and 30 seconds at 60 °C. The expression levels of GAPDH or U6 were used as internal standards. Additionally, the expression levels of viral genes were corrected based on the copy number of the viral genomic DNA.

Table 1. RT-qPCR primer sequences.

Gene Name	Forward primer (5'- -3')	Reverse primer (5'- -3')
BART	GGCTGTTCCTGAACGACGAG	CTATAGGCGCATCCTGCTGA
miR-BART4-5p	GACCTGATGCTGCTGGTGTGCT	mRQ 3'primer
miR-BART20-5p	TAGCAGGCATGTCTTCATTCC	mRQ 3'primer
BZLF1	TCCGACTGGGTCGTGGTT	GCTGCATAAGCTTGATAAGCATTC
BALF5	TAGGGCCAGTCAAAGTTG	ACCTGCGAAGACATAGAG
BALF4	AACCTTTGACTCGACCATCG	ACCTGCTCTTCGATGCACTT
EBNA1	GGTCGTGGACGTGGAGAAAA	GGTGGAGACCCGGATGATG
EBER1	CTACGCTGCCCTAGAGGTTTT	CAGCTGGTACTTGACCGAAGA
CASZ1a	GGATGCTGAGACAGATGAGTGC	CTGTCGGCATAGAGATGGTGTT
OCT1	ATGAACAATCCGTCAGAAACCAG	GATGGAGATGTCCAAGGAAAGC
ARID2	CAGTGTGTCGGATTATCTGCG	GCATGACGTGCTTGCTTTCATT
TP53INP1	TTCCTCCAACCAAGAACCAGA	GCTCAGTAGGTGACTCTTCACT
5.8S rRNA	GTCTACGCCATACCCT	AAAGCCTACAGCACCCGTA

2.7 Western Blotting

Approximately 1×10^6 cells were seeded into a 10 cm dish and treated with 0.1% DMSO or 2.5 μM SAHA. After 16 or 48 hours, the cells were lysed using RIPA buffer (ThermoFisher Scientific) supplemented with protease inhibitor (cOmplete mini, Sigma-Aldrich). Protein samples (5 μg) were electrophoresed using 15% SDS-PAGE, then transferred to a PVDF membrane (Merk Millipore, Brea, CA). The PVDF membrane was treated with Block ACE (KAC, Amagasaki, Japan) to prevent non-specific antibody binding. Subsequently, specific antibodies for TP53INP1 (EPR17974, Abcam, Danvers, MA), caspase-3 (W20054B; Biolegend, San Diego, CA), cleaved caspase-3 (Asp175) (5A1E; Cell Signaling Technology (CST), Danvers, MA) and GAPDH (EPR16891; Abcam) were incubated with the PVDF membrane. After washing, the membrane was incubated with horseradish peroxidase (HRP)-conjugated anti-rat IgG (Proteintech, Chicago, IL) or HRP-conjugated anti-rabbit IgG (CST). Specific antibody–antigen reactions were visualized using Immobilon (Merk Millipore) and detected with X-ray film. GAPDH expression levels were used as an internal standard.

2.8. DNA sequencing

Using cDNA synthesized from total RNA derived from MKN28 cells as a template, DNA was amplified by the MJ Research PTC-200 (Bio-Rad) machine using the primer set 5'-ACCTATGGAAACTACTTCCTGAAA-3' and 5'-GCAGGCCAACTTGTTCAGTG-3' and

KOD One polymerase. The amplified PCR product was used as a template for sequencing reactions with PCR primers or sequencing primers (5'-GTGTAACAGTTCCTGCATGGG-3' or 5'-CAAAGCTGTTCCGTCCCAGT-3') and BigDye Terminator v 3.1 (ThermoFisher), and analyzed with the 3500 Genetic Analyzer (ThermoFisher). The obtained results were analyzed using Snapgene Viewer (GSL Biotech, San Diego, CA) (**Supplementary 1**).

2.9. miRNA reporter assay

Using DNA extracted from AGS cells as a template, DNA was amplified with TP53INP1 3'untranslated region (3'UTR) specific primers (5'-TAGGCGATCGCTCGAGAGCTTGTTTT CTTGAGCCACGGTCT-3' and 5'-TTGCGGCCAGCGGCCGCGATTGAAAACTGTAACTC CAGGTAGTGCAA-3') and KOD One polymerase using the MJ Research PTC-200. Using the In-Fusion Snap Assembly Master Kit (TaKaRa), the amplified PCR product containing a miR-BART22-3p binding site was inserted into the *Not* I-*Xho* I digested psiCHECK-2 vector (Promega) which includes both Renilla and firefly luciferase reporter genes to construct the psiCHECK-2 TP53INP1 3'UTR vector. AGS cells or AGS EBV cells were seeded at 5 x 10^4 cells/well in each well of a 24-well plate. After 24 hours, 20 ng of vector alone, or 20 ng of vector with 20 nM negative control (mG/ZEN/mCmGmUmAmUmUmAmUmAmGmCmCmGmAm UmUmAmAmCmG/3ZEN/-3'), or miR-BART22-3p inhibitor (5'-mA/ZEN/ mCmUmAmCmU

mAmGmAmCmCmAmUmGmAmCmUmUmUmGmUmA/3ZEN/-3', synthesized by IDT), was introduced using Lipofectamine 2000 (ThermoFisher). After 48 hours of gene introduction, luciferase enzyme activity was quantified using the Dual-Luciferase Kit (Promega) and the GloMax Navigator (Promega). The enzyme activity values were normalized to the negative control values, and then the measurements of AGS EBV cells were compared with those of EBV-negative AGS cells.

2.10. Statistical analysis

The Mann-Whitney U test was employed to analyze whether there was a difference between two independent groups. The data were presented as mean ± standard deviation (SD). Statistical significance was set at $p < 0.05$.

3. Results

3.1. SAHA suppresses the activity of the BART gene promoter and inhibits the expression of BART miRNAs

It has been reported that dasatinib (Kotaki et al., 2020, Dargart et al., 2012), SAHA (Hui et al., 2012), rapamycin (Nepomuceno et al., 2003, Adamson et al., 2014), topotecan (Kawanishi, 1993, Wang et al., 2009), and ganciclovir (Hui et al., 2010, Westphal et al., 1999) have anti-EBV

activity. This study examined the impact of these drugs on BART promoter activity. Dasatinib and SAHA decreased BART promoter activity by less than 0.5-fold, while topotecan exhibited an increase of more than 1.5-fold (**Fig. 1A**). To evaluate the effect on EBV-positive cells, the expression of miR-BART4-5p was assessed after treatment with dasatinib and SAHA using RT-qPCR (**Supplementary 3A**). Dasatinib reduced the expression of miR-BART4-5p to 30% (**Fig. 1b**), while SAHA decreased it to 7% (**Fig. 1C)**. Moreover, SAHA also reduced the expression of miR-BART20-5p to 11% (**Fig. 1C**). Primers designed to amplify transcripts (BART, RPMS1, BRAF0, RK-BARF0, and miR-BARTs) regulated by the BART promoter (Edwards et al., 2008) were employed to measure BART transcript levels using the RT-qPCR method (**Supplementary 3B**). Following SAHA treatment, a time-dependent reduction in the expression of BART transcripts was observed (**Fig. 1D, black circle**). Additionally, the expression of miR-BART4-5p decreased after SAHA treatment (**Fig. 1D, white circle**). These findings indicate that SAHA not only suppresses BART promoter activity but also inhibits BART miRNA expression.

3.2. SAHA induces cell death in EBV-positive cells in a p53-independent manner

The impact of SAHA on EBV-positive epithelial cancers has been investigated using AGS, HK1, HONE1, and C666-1 cells with wild-type p53, yet the effects of SAHA on cells with mutant p53 remain unknown (Hui et al., 2010, Hui et al., 2012). The IC_{50} of SAHA was 3.9 μM for AGS

cells with wild-type p53 and 1.4 μM for AGS EBV cells, showing a 2.8-fold increase in drug sensitivity upon EBV infection (Fig. 2A, left). In the MKN28 cell line, isoleucine at position 251 of the TP53 gene was replaced with leucine by the substitution from adenine to cytidine as reported previously (Matozaki et al., 1992) (**Supplementary 1**). As for cells with a p53 mutation, the IC_{50} of SAHA was 4.9 μM in MKN28 cells, whereas, it was 2.6 μM in MKN28 EBV cells, indicating a 1.9-fold increase in drug sensitivity due to EBV infection (**Fig. 2A, right**). The treatment of MKN28-EBV cells with SAHA reduced the expression of BART transcripts to 5% of that of the untreated cells (**Supplementary 4**). Furthermore, the treatment of AGS EBV cells with SAHA significantly elevated the expression levels of the immediate early gene BZLF1 and early gene BALF5 by more than 20-fold, and late gene BALF4 by approximately 8-fold (**Fig. 2B**). EBV genome copies began to rise 24 hours after SAHA treatment, escalating by 12 and 23 times after 48 and 72 hours, respectively (**Fig. 2C**). The increase in EBV copy number with SAHA treatment was 11-fold in our experiments, compatible with the 8-fold increase in a previous report (Hui et al., 2010). These findings indicate that SAHA treatment induces cell death specifically in EBV-positive cells, regardless of p53 mutation. Therefore, the viral status of EBV-positive cells moves from latent to lytic infection.

3.3. SAHA induces EBV-positive cell-specific cell death independent of lytic infection induction

As the enhanced cell death observed in the SAHA-treated EBV-positive cells could be attributed to the induction of lytic infection, experiments were performed using AGS BZLF1-KO EBV cells, in which EBV never shifts to lytic infection. The IC_{50} for SAHA was 3.9 μM for AGS cells and 1.7 μM for AGS BZLF1-KO EBV cells, indicating that AGS BZLF1-KO EBV-infected cells were 2.3-fold more sensitive to SAHA than uninfected AGS cells (**Fig. 3A**). AGS BZLF1-KO EBV cells showed approximately 30% lower expression of the early BALF5 and late BALF4 genes after 48 hours of SAHA treatment, compared to AGS EBV cells (**Fig. 3B**). After 72 hours of treatment with SAHA, the number of BZLF1-KO EBV genome copies increased by only 1.5 times (**Fig. 3C**).

To determine the extent to which SAHA treatment induces apoptosis in cells, the number of cells stained with 7-AAD and Annexin V was measured using a flow cytometer. A population of cells exhibiting forward scatter and side scatter within a certain range was gated and extracted (**Supplementary 2A**), and the number of cells undergoing early and late apoptosis within this population was counted (**Supplementary 2B**). The same experiment was repeated three times, and the sum of the cells undergoing early and late apoptosis was calculated, with the mean value and standard deviation presented (**Fig. 3D**). The total number of apoptotic cells in the AGS cells treated with SAHA increased by 1.9 times, from 3.4% to 6.5% (**Fig. 3D**). Conversely, the total number of apoptotic cells in the AGS EBV cells treated with SAHA increased by 3.7 times, from

7.7% to 28.4 % (**Fig. 3D**). The treatment with SAHA for 48 hours elevated the number of cells in early apoptosis by 3.6 times, from 6.9% to 24.8%, in AGS BZLF1-KO EBV cells (**Fig. 3D**). Compared to AGS cells, AGS EBV cells or AGS BZLF1-KO EBV cells exhibited a higher frequency of apoptosis upon SAHA treatment. However, there was no significant difference in the frequency of apoptosis between AGS EBV cells and AGS BZLF1-KO EBV cells (**Fig. 3D**).

These findings indicate that SAHA induces apoptosis in EBV-infected cells without triggering lytic infection.

3.4. SAHA suppresses the transcription of BART miRNAs and enhances the expression of BART miRNA target genes

As SAHA induced cell death in EBV-positive cells under conditions that did not induce lytic infection (**Fig. 3B and 3C**), we investigated the changes in the expression of viral latent genes associated to the SAHA treatment. In AGS EBV cells treated with SAHA, the expression of the latent genes BART, EBNA1, and EBER1 decreased by 85%, 15%, and 22%, respectively, compared to untreated cells (**Fig. 4A, left**). In SAHA-treated AGS BZLF1-KO EBV cells, the expression of BART and EBER1 decreased by 66% and 25%, respectively, compared to untreated cells. However, the expression of EBNA1 was not significantly different between SAHA-treated and untreated AGS BZLF1-KO EBV cells (**Fig. 4A, right**).

The BART miRNAs target genes involved in promoting apoptosis include CASZ1a, OCT1, TP53INP1, and ARID2 (Kang et al., 2015). The 3'UTR region of the TP53INP1 gene, which contains the target site for miR-BART22-3p, was inserted downstream of the firefly luciferase gene to create the psiCHECK-2-TP53INP1 3'UTR vector. When this miRNA assay vector was introduced into AGS cells and EBV AGS cells, the luciferase activity in EBV AGS cells was only 40% of that in AGS cells (**Supplementary 5, left**). Furthermore, when the miRNA assay vector and the miR-BART22-3p inhibitor were simultaneously introduced into the cells, the luciferase activity in EBV-positive cells increased 7-fold compared to EBV-negative cells (**Supplementary 5, right**). In AGS EBV cells which produce BART miRNAs, the expression of these apoptosis-inducing genes significantly decreased, ranging from 43% to 87%, when compared to non-infected AGS cells (**Fig. 4B**). To the contrary, when AGS EBV cells were treated with SAHA for 16 hours, the expression of CASZ1a, OCT1, and TP53INP1 increased by 1.9-fold, 1.5-fold, and 1.3-fold, respectively, compared to untreated cells, while ARID2 was reduced to 50% of the level expressed in untreated cells (**Fig. 4C, middle)**. The SAHA treatment increased the expression of OCT1 and TP53INP1 in BZLF1-KO EBV-infected cells similar to wild-type EBV-infected cells (**Fig. 4C, left**). On the other hand, the SAHA treatment did not increase the expression of OCT1 or TP53INP1 in uninfected AGS cells (**Fig. 4C, right**).

Furthermore, in AGS EBV cells treated with SAHA, TP53INP1 protein expression increased at 16 hours and 48 hours, but the expression was stronger at 16 hours than at 48 hours. The expression of active caspase-3, a marker of apoptosis, was observed at a slightly higher level at 16 hours and more strongly at 48 hours after SAHA treatment (**Fig. 4D**). Similarly, in AGS EBV BZLF1 KO cells treated with SAHA, the increased levels of TP53INP1 and active caspase-3 were stronger at 16 hours than at 48 hours (**Supplementary 6**). These findings suggest that SAHA induces cell death through suppressing the expression of viral miRNAs and promoting the expression of genes that induce apoptosis.

4. Discussion

We discovered that SAHA, which is clinically used as an HDAC inhibitor, inhibits BART promoter activity. The treatment of nasopharyngeal cancer cells with SAHA enhanced the expression of EBV lytic genes and induced cell death in infected cells (Hui et al., 2010). SAHA also increased cell death in SNT13, SNT16, and KAI3 cells derived from EBV-positive NK/T lymphomas; however, SAHA did not induce lytic infection in SNT16 and KAI3 cells (Siddiquey et al., 2014). We showed that SAHA significantly increased cell apoptosis in gastric epithelial cells infected with BZLF1-KO EBV, which never undergo lytic infection, compared to uninfected

gastric epithelial cells (**Fig. 3**). These findings suggest that the cytotoxic effect of SAHA on EBV-positive cells involves a different mechanism than the induction of EBV lytic genes.

Our study revealed that treating cells with SAHA reduced the expression of the BART gene in EBV BZLF1-KO-infected gastric epithelial cells (**Fig. 4A, right**). BART miRNAs are known to exhibit anti-apoptotic functions (Kang et al., 2015; Lin et al., 2015; Min et al., 2020). Conversely, apoptotic signals have been reported to induce the expression of EBV lytic infection genes (Murata et al., 2021). Therefore, we hypothesize that SAHA induces apoptosis in infected cells through the suppression of BART promoter activity, even when the expression of EBV lytic infection genes is not induced. The detailed analysis of BART promoter activity and experiments involving the suppression of BART promoter activity using CRISPR interference will be necessary to elucidate this molecular mechanism (Kim et al., 2019; Mandegar et al., 2016).

In EBV infection, infected cells receive signals that trigger apoptosis. However, EBV latent genes provide rescue signals to stressed cells, preventing apoptotic cell death (Iizasa et al., 2012, Tsao et al., 2017). The BART miRNAs expressed during latent infection suppress the activity of various apoptosis-inducing genes (Kang et al., 2015, Lin et al, 2015, Min et al., 2020). As EBV-infected epithelial cells have higher BART miRNA expression compared to B lymphoma cells (Marquitz et al., 2015), the strong suppression of BART miRNA expression by SAHA may induce apoptosis in EBV-positive epithelial cancers. miRNAs strongly suppress protein

expression despite not strongly inhibiting messenger RNA (mRNA) expression (Bartel 2018). Upon SAHA treatment, the expression of CASZ1a and TP53INP1 decreased by more than 50% in EBV-infected cells compared to uninfected cells (**Fig. 4B**). Because miRNAs promote the degradation of mRNA by de-polyadenylating the targeted mRNA (Bartel 2018), mRNAs with shorter polyA tails are more susceptible to miRNA-mediated degradation (Eulalio et al., 2009). Additionally, the expression of p53 is strongly suppressed by deadenylation (Zhang et al., 2015). These reasons suggest that the expression of CASZ1a and TP53INP1 was inhibited by more than 50% due to miRNA activity.

On the other hand, the expression of EBNA1 and EBER, which were latent EBV genes, was hardly affected by SAHA treatment (**Fig. 4A**). In EBV-positive gastric cancer cells, EBNA1 is continuously expressed through the activity of the Q promoter (Tao et al., 1998), and EBER is continuously expressed due to RNA polymerase III activity (Howe & Shu, 1989). It is known that housekeeping genes can be continuously expressed, because the lysine residues at the N-terminus of histones bound to their promoters are frequently acetylated (She et al., 2009). We assume these viral genes may be regulated in a similar manner.

HDAC inhibitors typically enhance the expression of various genes through preventing histones from binding to DNA (Falkenberg & Johnstone., 2014, Seto & Yoshida, 2014). However, SAHA, despite being an HDAC inhibitor, has been observed to reduce the expression of viral

LMP1 and host c-Myc genes in EBV-positive DLBCL (Shin et al., 2014). Additionally, SAHA recruits inhibitors to the promoter of the telomerase reverse transcription enzyme (TERT) and suppresses TERT expression in lung cancer cells (Li et al., 2011, Rahman & Grundy, 2011). Therefore, even though SAHA is classified as an HDAC inhibitor, it is believed to suppress BART gene activity through either increasing the expression of transcriptional inhibitors or recruiting these inhibitors to the BART promoter.

We demonstrated a remarkable similarity in both the IC_{50} value and the capacity to induce apoptosis between wild-type EBV- and EBV BZLF1-KO-infected cells when exposed to SAHA, as illustrated in **Fig. 2** and **Fig. 3**. However, SAHA enhanced apoptosis independently of EBV lytic infection (**Fig. 3B**). Furthermore, the rate of apoptosis in SAHA-treated both EBV-infected cells and EBV BZLF1-KO-infected cells was similar (**Fig. 3D**), so we believe that the anti-EBV effect of SAHA is likely mediated by the decrease in BART miRNA expression. Consequently, SAHA not only triggers cell death in EBV-positive cells through lytic infection, but also amplifies apoptosis through suppressing the expression of BART miRNAs. Variants of EBV lacking various viral lytic genes have been associated with numerous instances of lymphomas and epithelial cancers (Okuno et al., 2019, Kondo et al., 2022, Wongwiwat et al., 2022). Consequently, SAHA is anticipated to exhibit potent antitumor effects against EBV-associated cancers in which it is difficult to induce apoptosis solely through inducing lytic infection.

5. Conclusion

This study demonstrated that the HDAC inhibitor SAHA induces cell death in EBV-positive cells both with and without leading to lytic infection. SAHA was also shown to have efficacy in p53 mutant EBV-positive gastric cancer cells. Given that certain EBV-related tumors lack p53 mutations and are infected with an EBV strain that never exhibits lytic infection, this drug could be effective for the treatment of various EBV-associated cancers.

Contributor roles

Yuxin Liu: formal analysis, investigation, writing original draft preparation, writing, reviewing and editing.

Aung Phyo Wai: Formal analysis, investigation.

Tumurgan Zolzaya: Investigation.

Yuichi Iida: Investigation.

Shunpei Okada: Investigation.

Hisashi Iizasa: Conceptualization, writing original draft preparation, writing, reviewing and editing, supervision.

Hironori Yoshiyama: Conceptualization, writing original draft preparation, writing, reviewing and editing, supervision. All authors have read and agreed to the published version of the manuscript.

Funding

This research was funded by the Ministry of Education, Culture, Sports, Science, and Technology's Scientific Research Fund [22K07101 (HI) and 21K07054 (YH)] and JST SPRING [JPMJSP2155] (YL).

Conflicts of Interest

The authors declare no conflicts of interest.

Acknowledgments

We would like to thank Editage (www.editage.com) for English language editing. The authors also thank the technological expertise of the Interdisciplinary Center for Science Research, Organization for Research and Academic Information, Shimane University.

References

Adamson, A.L., Le, B.T., Siedenburg, B.D. 2014. Inhibition of mTORC1 inhibits lytic replication of Epstein-Barr virus in a cell-type specific manner. Virol. J. 11, 110. https://doi.org/10.1186/1743-422X-11-110

Bartel, D.P. 2018. Metazoan MicroRNAs. Cell 173, 20-51. https://doi.org/10.1016/j.cell.2018.03.006

Cai, X., Schäfer, A., Lu, S., Bilello, J.P., Desrosiers, R.C., Edwards, R., Raab-Traub, N., Cullen, B.R. 2006. Epstein-Barr virus microRNAs are evolutionarily conserved and differentially expressed. PLoS Pathog. 2, e23. https://doi.org/10.1371/journal.ppat.0020023

Chen, H., Huang, J., Wu, F.Y., Liao, G., Hutt-Fletcher, L., Hayward, S.D. 2005. Regulation of expression of the Epstein-Barr virus BamHI-A rightward transcripts. J. Virol. 79, 1724-1733. https://doi.org/10.1128/JVI.79.3.1724-1733.2005

Countryman, J., Miller, G. 1985. Activation of expression of latent Epstein-Barr herpesvirus after gene transfer with a small cloned subfragment of heterogeneous viral DNA. Proc. Natl. Acad. Sci. U. S. A. 82, 4085-4089. https://doi.org/10.1073/pnas.82.12.4085

Daigle, D., Gradoville, L., Tuck, D., Schulz, V., Wang'ondu, R., Ye, J., Gorres, K., Miller, G. 2011. Valproic acid antagonizes the capacity of other histone deacetylase inhibitors to activate the Epstein-barr virus lytic cycle. J. Virol. 85, 5628-5643. https://doi.org/ 10.1128/JVI.02659-10

Dargart, J.L., Fish, K., Gordon, L.I., Longnecker, R., Cen, O. 2012. Dasatinib therapy results in decreased B cell proliferation, splenomegaly, and tumor growth in a murine model of lymphoma expressing Myc and Epstein-Barr virus LMP2A. Antivir. Res. 95, 49–56. https://doi.org/10.1016/j.antiviral.2012.05.003

De Jesus, O., Smith, P.R., Spender, L.C., Elgueta Karstegl, C., Niller, H.H., Huang, D., Farrell, P.J. 2003. Updated Epstein-Barr virus (EBV) DNA sequence and analysis of a promoter for the BART (CST, BARF0) RNAs of EBV. J. Gen. Virol. 84, 1443-1450. https://doi.org/ 10.1099/vir.0.19054-0

De Re, V., Caggiari, L., De Zorzi, M., Fanotto, V., Miolo, G., Puglisi, F., Cannizzaro, R., Canzonieri, V., Steffan, A., Farruggia, P., Lopci, E., d'Amore, E.S.G., Burnelli, R., Mussolin, L., Mascarin, M. 2020. Epstein-Barr virus BART microRNAs in EBV- associated Hodgkin lymphoma and gastric cancer. Infect. Agent. Cancer. 15, 42. https://doi.org/10.1186/ s13027 -020-00307-6

Edwards, R.H., Marquitz, A.R., Raab-Traub, N. 2008. Epstein-Barr virus BART microRNAs are produced from a large intron prior to splicing. J. Virol. 82, 9094-9106. https://doi.org/ 10.1128/JVI.00785-08

Eulalio, A., Huntzinger, E., Nishihara, T., Rehwinkel, J., Fauser, M., Izaurralde, E. 2009. Deadenylation is a widespread effect of miRNA regulation. RNA 15:21-32. https://doi.org/10.1261/rna.1399509

Falkenberg, K.J., Johnstone, R.W. 2014. Histone deacetylases and their inhibitors in cancer, neurological diseases and immune disorders. Nat. Rev. Drug Discov. 13, 673-691. https://doi.org/10.1038/nrd4360

Gelmini, S., Orlando, C., Sestini, R., Vona, G., Pinzani, P., Ruocco, L., Pazzagli, M.1997. Quantitative polymerase chain reaction-based homogeneous assay with fluorogenic probes to measure c-erbB-2 oncogene amplification. Clin. Chem. 43, 752-758.

Hall, M.P., Unch, J., Binkowski, B.F., Valley, M.P., Butler, B.L., Wood, M.G., Otto, P., Zimmerman, K., Vidugiris, G., Machleidt, T., Robers, M.B., Benink, H.A., Eggers, C.T., Slater, M.R., Meisenheimer, P.L., Klaubert, D.H., Fan, F., Encell, L.P., Wood, K.V. 2012. Engineered luciferase reporter from a deep sea shrimp utilizing a novel imidazopyrazinone substrate. ACS Chem. Biol. 7, 1848-185. https://doi.org/10.1021/cb3002478

Howe, J.G., Shu, M.D. 1989. Epstein-Barr virus small RNA (EBER) genes: unique transcription units that combine RNA polymerase II and III promoter elements. Cell 57:825-834. https://doi.org/ 10.1016/0092-8674(89)90797-6.

Hui, K.F., Chiang, A.K. 2010. Suberoylanilide hydroxamic acid induces viral lytic cycle in Epstein-Barr virus-positive epithelial malignancies and mediates enhanced cell death. Int. J. Cancer 126, 2479-2489. https://doi.org/10.1002/ijc.24945

Hui, K.F., Ho, D.N., Tsang, C.M., Middeldorp, J.M., Tsao, G.S., Chiang, A.K. 2012. Activation of lytic cycle of Epstein-Barr virus by suberoylanilide hydroxamic acid leads to apoptosis and tumor growth suppression of nasopharyngeal carcinoma. Int. J. Cancer. 131, 1930-1940. https://doi.org/10.1002/ijc.27439

Iizasa, H., Kim, H., Kartika, A.V., Kanehiro, Y., Yoshiyama, H. 2020. Role of Viral and Host microRNAs in Immune Regulation of Epstein-Barr Virus-Associated Diseases. Front. Immunol. 11, 367. https://doi.org/ 10.3389/fimmu.2020.00367

Iizasa, H., Nanbo, A., Nishikawa, J., Jinushi, M., Yoshiyama, H. 2012. Epstein-Barr Virus (EBV)-associated gastric carcinoma. Viruses 4, 3420-3439. https://doi.org/10.3390/v4123420

Ishiyama, M., Tominaga, H., Shiga, M., Sasamoto, K., Ohkura, Y., Ueno, K. 1996. A combined assay of cell viability and in vitro cytotoxicity with a highly water-soluble tetrazolium salt, neutral red and crystal violet. Biol. Pharm. Bull. 19, 1518-1520. https://doi.org/10.1248/bpb.19.1518

Kanda, T., Miyata, M., Kano, M., Kondo, S., Yoshizaki, T., Iizasa, H. 2015. Clustered microRNAs of the Epstein-Barr virus cooperatively downregulate an epithelial cell-specific metastasis suppressor. J. Virol. 89, 2684-2697. https://doi.org/10.1128/JVI.03189-14

Kang, D., Skalsky, R.L., Cullen, B.R. 2015. EBV BART MicroRNAs Target Multiple Pro-apoptotic Cellular Genes to Promote Epithelial Cell Survival. PLoS Pathog. 11, e1004979. https://doi.org/10.1371/journal.ppat.1004979

Kartika, A.V., Iizasa, H., Ding, D., Kanehiro, Y., Tajima, Y., Kaji, S., Yanai, H., Yoshiyama, H. 2020. Application of Biopsy Samples Used for *Helicobacter pylori* Urease Test to Predict Epstein-Barr Virus-Associated Cancer. Microorganisms 8, 923. https://doi.org/10.3390/microorganisms8060923

Katsumura, K.R., Maruo, S., Wu, Y., Kanda, T., Takada, K. 2009. Quantitative evaluation of the role of Epstein-Barr virus immediate-early protein BZLF1 in B-cell transformation. J. Gen. Virol. 90, 2331-2341. https://doi.org/10.1099/vir.0.012831-0

Kawanishi, M. 1993. Topoisomerase I and II activities are required for Epstein-Barr virus replication. J. Gen. Virol. 74, 2263-2268. https://doi.org/10.1099/0022-1317-74-10-2263

Kawanishi, M. 1993. Epstein-Barr virus induces fragmentation of chromosomal DNA during lytic infection. J. Virol. 67, 7654-7658. doi: 10.1128/JVI.67.12.7654-7658.1993

Kim, D.N., Song, Y.J., Lee, S.K. 2011. The role of promoter methylation in Epstein-Barr virus (EBV) microRNA expression in EBV-infected B cell lines. Exp. Mol. Med. 43, 401-410. https://doi.org/10.3858/emm.2011.43.7.044

Kim, H., Burassakarn, A., Kang, Y., Iizasa, H., Yoshiyama, H. 2019. A single nucleotide polymorphism in BART promoter region of Epstein-Barr virus isolated from nasopharyngeal cancer cells. Biochem. Biophys. Res. Commun. 520, 373-378. https://doi.org/10.1016/j.bbrc.2019.10.028

Klinke, O., Feederle, R., Delecluse, H.J. 2014. Genetics of Epstein-Barr virus microRNAs. Semin Cancer Biol. 26, 52-59. https://doi.org/10.1016/j.semcancer.2014.02.002

Kondo, S., Okuno, Y., Murata, T., Dochi, H., Wakisaka, N., Mizokami, H., Moriyama-Kita, M., Kobayashi, E., Kano, M., Komori, T., Hirai, N.;, Ueno, T., Nakanishi, Y., Endo, K., Sugimoto, H., Kimura, H., Yoshizaki, T. 2022. EBV genome variations enhance clinicopathological features of nasopharyngeal carcinoma in a non-endemic region. Cancer Sci. 113, 2446-56

Kotaki, R., Kawashima, M., Yamamoto, Y., Higuchi, H., Nagashima, E., Kurosaki, N., Takamatsu, M., Kikuti, Y.Y., Imadome, KI., Nakamura, N., Kotani, A. 2020. Dasatinib exacerbates splenomegaly of mice inoculated with Epstein-Barr virus-infected lymphoblastoid cell lines. Sci. Rep. 10, 7102. https://doi.org/10.1038/s41598-020-63901-z

Li, C.T., Hsiao, Y.M., Wu, T.C., Lin, Y.W., Yeh, K.T., Ko, J.L. 2011. Vorinostat, SAHA, represses telomerase activity via epigenetic regulation of telomerase reverse transcriptase in non-small cell lung cancer cells. J. Cell Biochem. 112, 3044-3053. https://doi.org/10.1002/jcb.23229

Lin, X., Tsai, M.H., Shumilov, A., Poirey, R., Bannert, H., Middeldorp, J.M., Feederle, R., Delecluse, H.J. 2015. The Epstein-Barr Virus BART miRNA cluster of the M81 strain

modulates multiple functions in primary B cells. PLoS Pathog. 11, e1005344. https://doi.org/10.1371/journal.ppat.1005344

Mandegar, M.A., Huebsch, N., Frolov, E.B., Shin, E., Truong, A., Olvera, M.P., Chan, A.H., Miyaoka, Y., Holmes, K., Spencer, C.I., Judge, L.M., Gordon, D.E., Eskildsen, T.V., Villalta, J.E., Horlbeck, M.A., Gilbert, L.A., Krogan, N.J., Sheikh, S.P., Weissman, J.S., Qi, L.S., So, P.L., Conklin, B.R. 2016. CRISPR Interference Efficiently Induces Specific and Reversible Gene Silencing in Human iPSCs. Cell Stem Cell. 18, 541-553. https://doi.org/10.1016/j.stem.2016.01.022

Maruo, S., Yang, L., Takada, K. 2001. Roles of Epstein-Barr virus glycoproteins gp350 and gp25 in the infection of human epithelial cells. J. Gen. Virol. 82, 2373-2383. https://doi.org/10.1099/0022-1317-82-10-2373

Marquitz, A.R., Mathur, A., Edwards, R.H., Raab-Traub, N. 2015. Host Gene Expression Is Regulated by Two Types of Noncoding RNAs Transcribed from the Epstein-Barr Virus BamHI A Rightward Transcript Region. J. Virol. 89, 11256-11268. https://doi.org/10.1128/JVI.01492-15

Matozaki, T., Sakamoto, C., Matsuda, K., Suzuki, T., Konda, Y., Nakano, O., Wada, K., Uchida, T, Nishisaki, H., Nagao, M., Kasuga, M. 1992. Missense mutations and a deletion of the p53 gene in human gastric cancer. Biochem. Biophys. Res. Commun. 182, 215-223. https://doi.org/10.1016/s0006-291x(05)80133-0

Min, K., Kim, J.Y., Lee, S.K. 2020. Epstein-Barr virus miR-BART1-3p suppresses apoptosis and promotes migration of gastric carcinoma cells by targeting DAB2. Int. J. Biol. Sci. 16, 694-707. https://doi.org/10.7150/ijbs.36595

Murata, T., Sugimoto, A., Inagaki, T., Yanagi, Y., Watanabe, T., Sato, Y., Kimura, H., 2021. Molecular Basis of Epstein-Barr Virus Latency Establishment and Lytic Reactivation. Viruses 13, 2344. https://doi.org/10.3390/v13122344

Münz, C. 2019. Latency and lytic replication in Epstein-Barr virus-associated oncogenesis. Nat. Rev. Microbiol. 17, 691-700. https://doi.org/10.1038/s41579-019-0249-7

Nepomuceno, R.R., Balatoni, C.E., Natkunam, Y., Snow, A.L., Krams, S.M., Martinez, O.M. 2003. Rapamycin inhibits the interleukin 10 signal transduction pathway and the growth of Epstein Barr virus B-cell lymphomas. Cancer Res. 63, 4472-4480.

Nishitsuji, H., Harada, K., Ujino, S., Zhang, J., Kohara, M., Sugiyama, M., Mizokami, M., Shimotohno, K., 2018. Investigating the hepatitis B virus life cycle using engineered reporter hepatitis B viruses. Cancer Sci. 109, 241-249. https://doi.org/10.1111/cas.13440.

Okuno, Y., Murata, T., Sato, Y., Muramatsu, H., Ito, Y., Watanabe, T., Okuno, T., Murakami, N., Yoshida, K., Sawada, A., Inoue, M., Kawa, K., Seto, M., Ohshima, K., Shiraishi, Y., Chiba, K., Tanaka, H., Miyano, S., Narita, Y., Yoshida, M., Goshima, F., Kawada, J.I., Nishida, T., Kiyoi, H., Kato, S., Nakamura, S., Morishima, S., Yoshikawa, T., Fujiwara, S., Shimizu, N., Isobe, Y., Noguchi, M., Kikuta, A., Iwatsuki, K., Takahashi, Y., Kojima, S., Ogawa, S., Kimura, H., 2019. Defective Epstein-Barr virus in chronic active infection and haematological malignancy. Nat. Microbiol. 4, 404-413. https://doi.org/10.1038/s41564-018-0334-0

Qiu, J., Cosmopoulos, K., Pegtel, M., Hopmans, E., Murray, P., Middeldorp, J., Shapiro, M., Thorley-Lawson, D.A., 2011. A novel persistence associated EBV miRNA expression profile is disrupted in neoplasia. PLoS Pathog. 7, e1002193. https://doi.org/10.1371/journal.ppat.1002193

Rahman, R., Grundy, R. 2011. Histone deacetylase inhibition as an anticancer telomerase-targeting strategy. Int. J. Cancer. 129, 2765-2774. https://doi.org/10.1002/ijc.26241

Schmid, I, Uittenbogaart, C.H., Giorgi, J.V. 1994. Sensitive method for measuring apoptosis and cell surface phenotype in human thymocytes by flow cytometry. Cytometry 15, 12-20. https://doi.org/10.1002/cyto.990150104

Seto, E., Yoshida, M. 2014. Erasers of histone acetylation: the histone deacetylase enzymes. Cold Spring Harb. Perspect. Biol. **6**, a018713. https://doi.org/10.1101/cshperspect.a018713

She, X., Rohl, C.A., Castle, J.C., Kulkarni, A.V., Johnson, J.M., Chen, R. 2009. Definition, conservation and epigenetics of housekeeping and tissue-enriched genes. BMC Genomics. 10, 269. https://doi.org/10.1186/1471-2164-10-269.

Shin, D.Y., Kim, A., Kang, H.J., Park, S., Kim, D.W., Lee, S.S. 2015. Histone deacetylase inhibitor romidepsin induces efficient tumor cell lysis via selective down-regulation of LMP1 and c-myc expression in EBV-positive diffuse large B-cell lymphoma. Cancer Lett. 364, 89-97. https://doi.org/10.1016/j.canlet.2015.03.016.

Siddiquey, M.N., Nakagawa, H., Iwata, S., Kanazawa, T., Suzuki, M., Imadome, K., Fujiwara, S., Goshima, F., Murata, T., Kimura, H. 2014. Anti-tumor effects of suberoylanilide hydroxamic acid on Epstein-Barr virus-associated T cell and natural killer cell lymphoma. Cancer Sci. 105, 713-722. https://doi.org/10.1111/cas.12418.

Tao, Q., Robertson, K.D., Manns, A., Hildesheim, A., Ambinder, R.F. 1998. The Epstein-Barr virus major latent promoter Qp is constitutively active, hypomethylated, and methylation sensitive. J Virol. 72, 7075-7083. https://doi.org/10.1128/JVI.72.9.7075-7083.1998.

Tsao, S.W., Tsang, C.M., Lo, K.W. 2017. Epstein-Barr virus infection and nasopharyngeal carcinoma. Philos Trans. R. Soc. Lond. B. Biol. Sci. 372, 20160270. https://doi.org/10.1098/rstb.2016.0270

Wang, P., Rennekamp, A.J., Yuan, Y., Lieberman, P.M. 2009. Topoisomerase I and RecQL1 function in Epstein-Barr virus lytic reactivation. J. Virol. **83**, 8090-8098. https://doi.org/ 10.1128/JVI.02379-08

Westphal, E.M., Mauser, A., Swenson, J., Davis, M.G., Talarico, C.L., Kenney, S.C. 1999. Induction of lytic Epstein-Barr virus (EBV) infection in EBV-associated malignancies using adenovirus vectors in vitro and in vivo. Cancer Res. 59, 1485-1491.

Wongwiwat, W., Fournier, B., Bassano, I., Bayoumy, A., Elgueta Karstegl, C., Styles, C., Bridges, R., Lenoir, C., BoutBoul, D., Moshous, D., Neven, B., Kanda, T., Morgan, R.G., White, R.E., Latour, S., Farrell, P.J. 2022. Epstein-Barr Virus genome deletions in Epstein-Barr virus-positive T/NK cell lymphoproliferative diseases. J. Virol. 96, e0039422. https://doi.org/10.1128/jvi.00394-22

Yang, H.J., Huang, T.J., Yang, C.F., Peng, L.X., Liu, R.Y., Yang, G.D., Chu, Q.Q., Huang, J.L., Liu, N., Huang, H.B., Zhu, Z.Y., Qian, C.N., Huang, B.J. 2013. Comprehensive profiling of Epstein-Barr virus-encoded miRNA species associated with specific latency types in tumor cells. Virol. J. 10, 314. https://doi.org/10.1186/1743-422X-10-314

Young, L.S., Yap, L.F., Murray, P.G. 2016. Epstein-Barr virus: more than 50 years old and still providing surprises. Nat. Rev. Cancer 16, 789-802. https://doi.org/10.1038/nrc.2016.92

Zhang, X., Devany, E., Murphy, M.R., Glazman, G., Persaud, M., Kleiman, F.E. 2015. PARN deadenylase is involved in miRNA-dependent degradation of TP53 mRNA in mammalian cells. Nucleic Acids Res. 43, 10925-10938. https://doi.org/10.1093/nar/gkv959

Figure legends.

Fig. 1. SAHA treatment of AGS EBV cells suppresses BART gene expression. A Changes in *BART* promoter activity 48 hours after various drug treatments. Gray squares indicate relative luciferase activity less than 0.5; white squares indicate activities stronger than 0.5, but weaker than 1.5 ; a black square indicates activity stronger than 1.5. BART promoter activity in cells treated with 2.5 μM dasatinib, SAHA, rapamycin, valproic acid, topotecan, and ganciclovir. The promoter activity of control cells treated with DMSO was set to 1.0. **B** Expression of miR-BART4-5p in cells treated with dasatinib. White column: control; black bars: 2.5 μM dasatinib. The miRNA expression levels were normalized to virus copy number and U6 expression level, and the control was set to 1.0. **C** Expression of miR-BART4-5p and miR-BART20-5p in cells

treated with SAHA. White bars: control; black bars: 2.5 μM SAHA. The miRNA expression levels were normalized to virus copy number and U6 expression level, and the control was set to 1.0. **D** SAHA treatment suppresses BART transcripts and miR-BART4-5p expression over time. The expression levels of genes in AGS EBV cells 6 hours after drug treatment were normalized to virus copy number and set to 1. **A** - **D** RT-qPCR was performed after 48 hours of drug treatment. Black circles: BART transcripts; white circles: miR-BART4-5p. *$p < 0.05$. **$p < 0.01$.

Fig. 2. SAHA treatment induces lytic infection and triggers apoptosis in EBV-positive cells. **A** EBV-positive cells treated with SAHA undergo cell death in a p53-independent manner. Open square: uninfected cells; closed square: EBV-positive cells. Left: AGS cells harboring wild-type p53; right: MKN28 cells harboring mutant p53. The survival rates of DMSO-treated cells were defined as 100%. **B** Expression of viral lytic genes in SAHA-treated AGS EBV cells: immediate early (BZLF1), early (BALF5), late (BALF4). White bars: control (DMSO); black bars: 2.5 μM SAHA. The expression level of the gene in EBV-positive cells treated with DMSO was set to 1. **C** Relative EBV copy number in AGS EBV cells treated with SAHA. The virus copy number of AGS EBV cells treated with DMSO was set to 1. **A** and **B** Cell proliferation assay, RT-qPCR, and apoptosis assays were performed 48 hours after drug treatment. All results were obtained from three different samples. *$p < 0.05$. **$p < 0.01$.

Fig. 3. SAHA treatment induces apoptosis in EBV-positive cells without activating lytic infection. **A** AGS BZLF1-KO EBV cells become more apoptotic than uninfected AGS cells after SAHA treatment. Open squares: uninfected cells; closed squares: BZLF1-KO EBV-positive cells. The survival rate of cells treated with DMSO was defined as 100%. **B** Expression of viral lytic genes in SAHA-treated AGS BZLF1-KO EBV cells: early (BALF5), late (BALF4). White bars: control (DMSO); black bars: 2.5 μM SAHA. The expression level of the gene in AGS BZLF1-KO EBV cells treated with DMSO was set to 1.0. **C** Relative EBV copy number in AGS BZLF1-KO EBV

cells treated with SAHA. The virus copy number of AGS BZLF1-KO EBV cells treated with DMSO was set to 1.0. **D** SAHA treatment enhances apoptosis in AGS EBV cells and AGS BZLF1-KO EBV cells compared to uninfected AGS cells. Apoptosis was defined as the sum of the number of cells in early apoptosis and late apoptosis. White bars: control (DMSO); black bars: 2.5 μM SAHA. **A**, **B**, and **D** Cell proliferation assay, RT-qPCR, and apoptosis assays were performed 48 hours after drug treatment. All results were obtained from three different samples. *$p < 0.05$. **$p < 0.01$. ns: not significant.

Fig. 4. SAHA treatment enhances the expression of BART miRNA target genes in EBV-positive cells. **A** Changes in latent gene expression in EBV-positive cells with SAHA treatment. Left: AGS EBV cells; right: AGS BZLF1-KO EBV cells. White bars: control (DMSO); black bars: 2.5 μM SAHA. The quantification of messenger RNA levels was conducted using RT-qPCR and the level of DMSO-treated control cells was set to 1.0 for normalization. RT-qPCR was performed 48 hours after drug treatment. **B** Expression levels of CASZ1a, OCT1, ARID2, TP53INP1 genes targeted by BART miRNAs in AGS and AGS EBV cells. White bars: AGS cells; hatched bars: AGS EBV cells. Levels of each messenger RNA were quantified with RT-qPCR and the expression level of AGS cells was set to 1.0. **C** Changes in the expression of BART miRNA target genes in AGS, AGS EBV, and AGS BZLF1-KO EBV cells after SAHA treatment. Levels of each messenger RNA were quantified with RT-qPCR and the level of DMSO-treated control cells was set to 1.0. White bars: control (DMSO); black bars: 2.5 μM SAHA. **D** Expression of TP53INP1 protein in AGS EBV cells after SAHA treatment. Protein expression was detected through Western blotting. The expression level of GAPDH was used as an internal standard. All results were obtained from three different samples. *$p < 0.05$. **$p < 0.01$.

Fig. 1

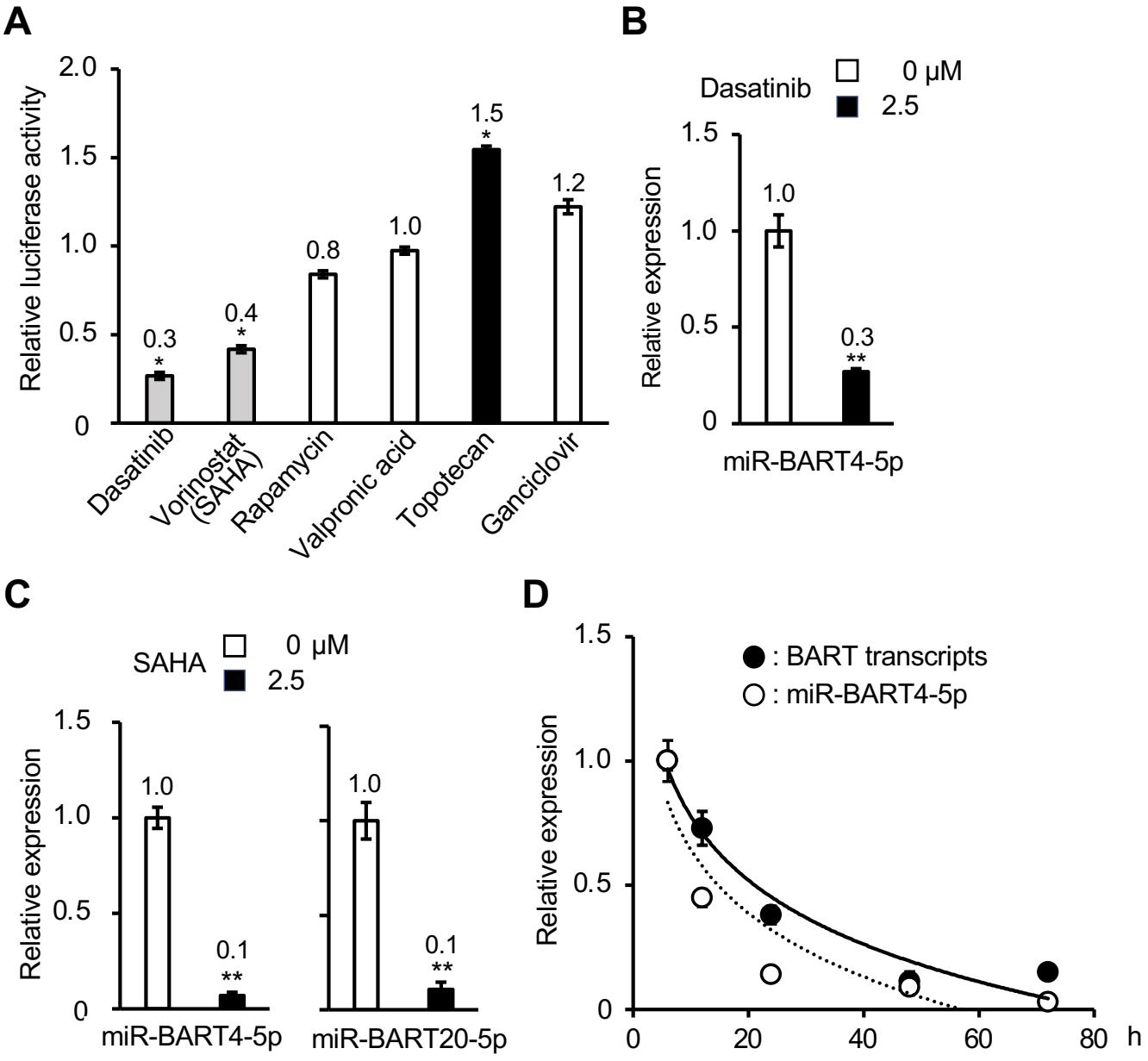
A
Relative luciferase activity
2.0
1.5
1.0
0.5
0
0.3
0.4
0.8
1.0
1.5
1.2
*
Dasatinib
Vorinostat (SAHA)
Rapamycin
Valpronic acid
Topotecan
Ganciclovir
B
Dasatinib
0 μM
2.5
Relative expression
1.0
0.3
**
miR-BART4-5p
C
SAHA
0 μM
2.5
Relative expression
1.0
0.1
**
miR-BART4-5p
miR-BART20-5p
D
: BART transcripts
: miR-BART4-5p
Relative expression
0
20
40
60
80
h

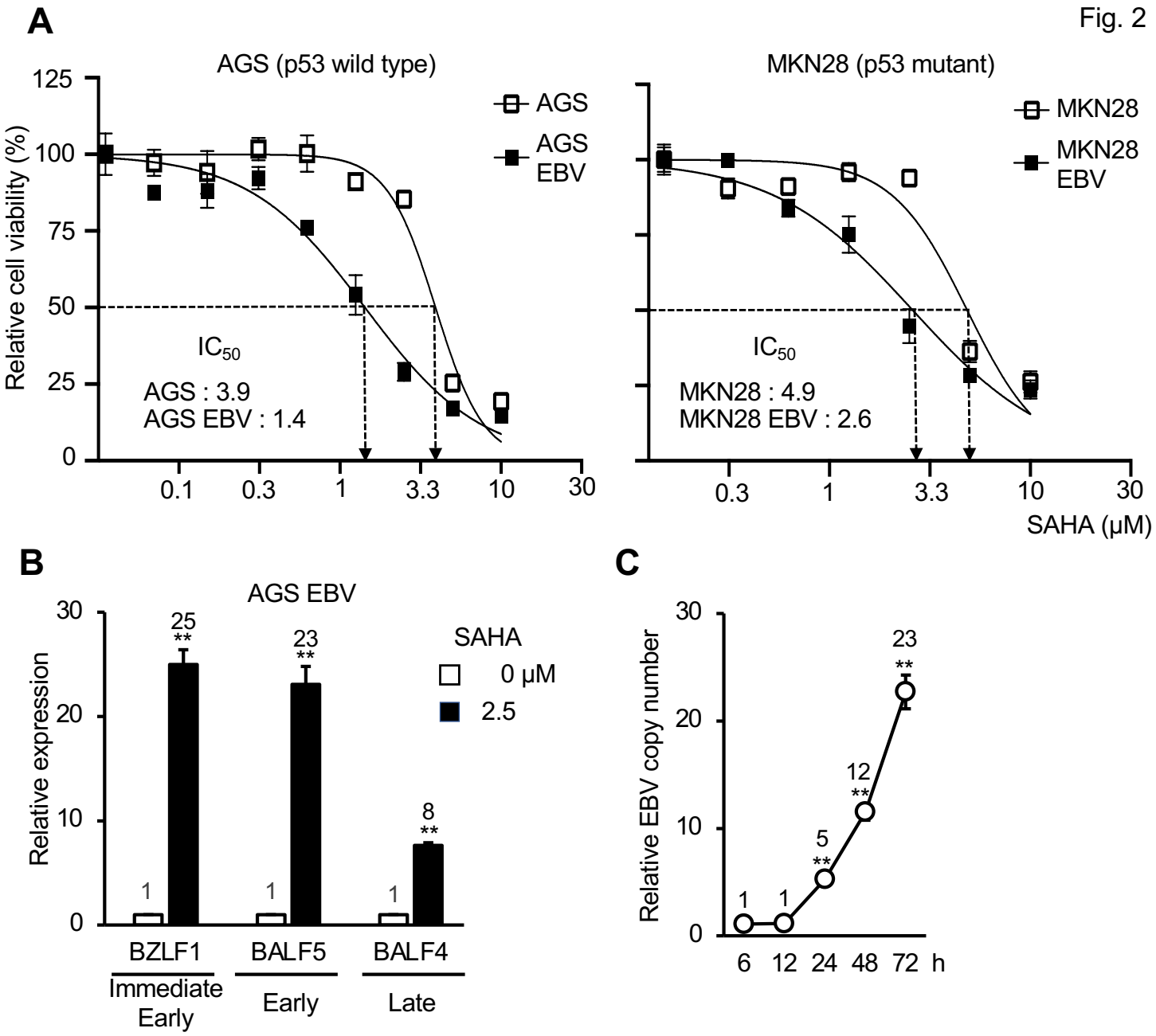
A
AGS (p53 wild type)
MKN28 (p53 mutant)
Relative cell viability (%)
AGS
AGS EBV
MKN28
MKN28 EBV
IC50
AGS : 3.9
AGS EBV : 1.4
MKN28 : 4.9
MKN28 EBV : 2.6
SAHA (μM)
B
AGS EBV
Relative expression
SAHA
0 μM
2.5
BZLF1
BALF5
BALF4
Immediate Early
Early
Late
C
Relative EBV copy number
h

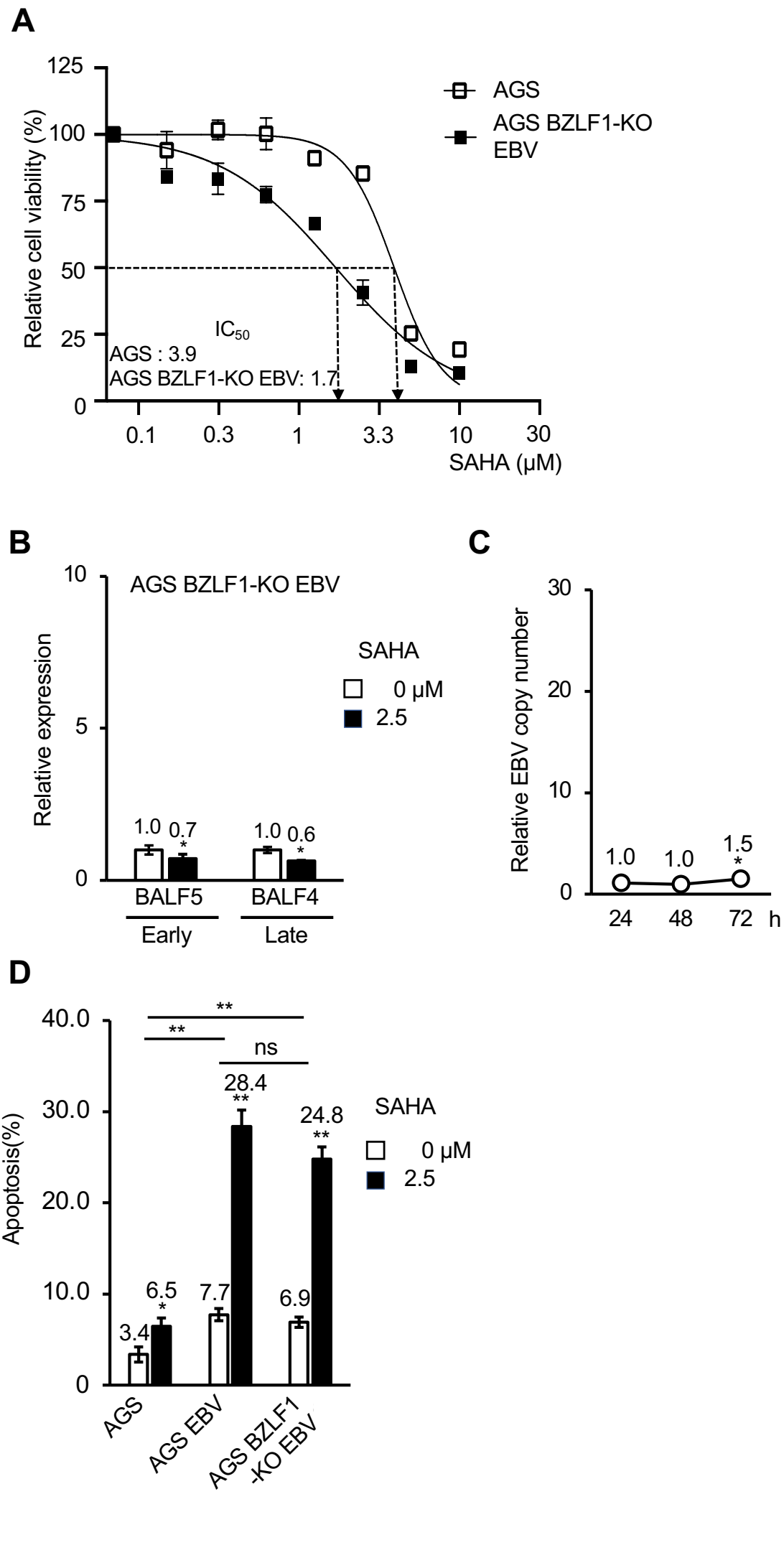
A
125
100
75
50
25
0
Relative cell viability (%)
AGS
AGS BZLF1-KO EBV
IC50
AGS : 3.9
AGS BZLF1-KO EBV: 1.7
0.1
0.3
1
3.3
10
30
SAHA (μM)
B
AGS BZLF1-KO EBV
Relative expression
10
5
0
SAHA
0 μM
2.5
1.0
0.7
1.0
0.6
BALF5
BALF4
Early
Late
C
Relative EBV copy number
30
20
10
0
1.0
1.0
1.5
24
48
72
h
D
Apoptosis(%)
40.0
30.0
20.0
10.0
0
**
**
ns
28.4
24.8
SAHA
0 μM
2.5
6.5
7.7
6.9
3.4
AGS
AGS EBV
AGS BZLF1 -KO EBV

Fig. 4

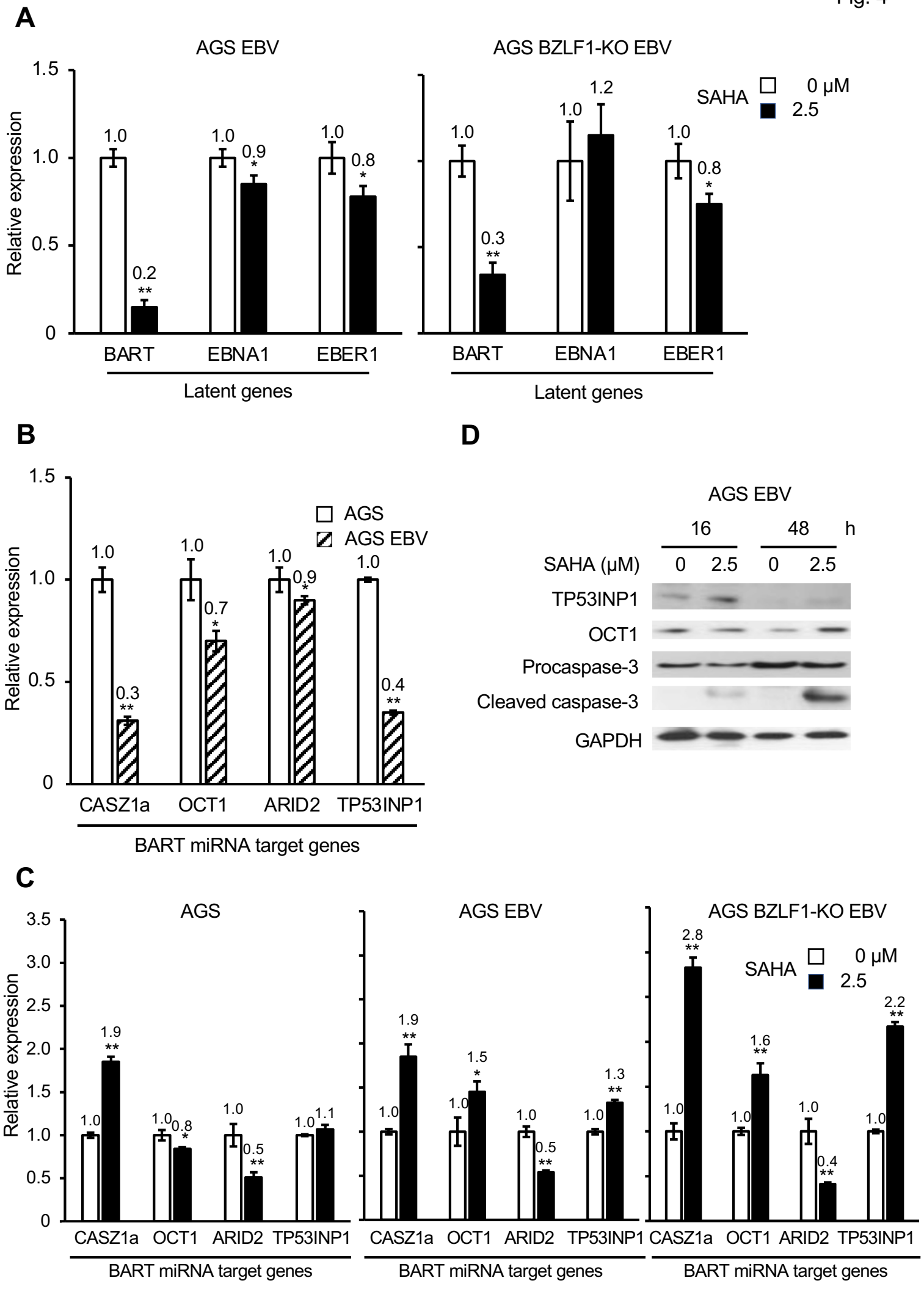
A
AGS EBV
AGS BZLF1-KO EBV
SAHA
0 μM
2.5
Relative expression
BART
EBNA1
EBER1
Latent genes
B
AGS
AGS EBV
CASZ1a
OCT1
ARID2
TP53INP1
BART miRNA target genes
D
AGS EBV
16
48
h
SAHA (μM)
TP53INP1
OCT1
Procaspase-3
Cleaved caspase-3
GAPDH
C
AGS
AGS EBV
AGS BZLF1-KO EBV

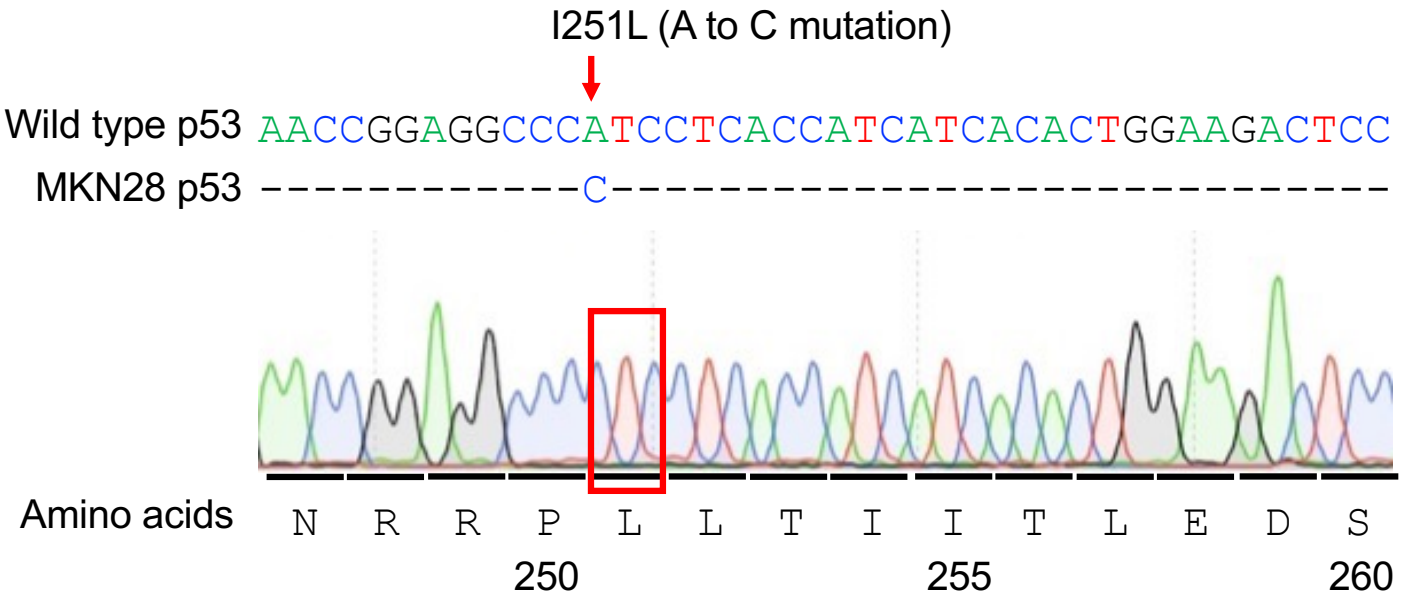

Supplementary 1

Partial DNA sequence of the TP53 gene in MKN28 cells

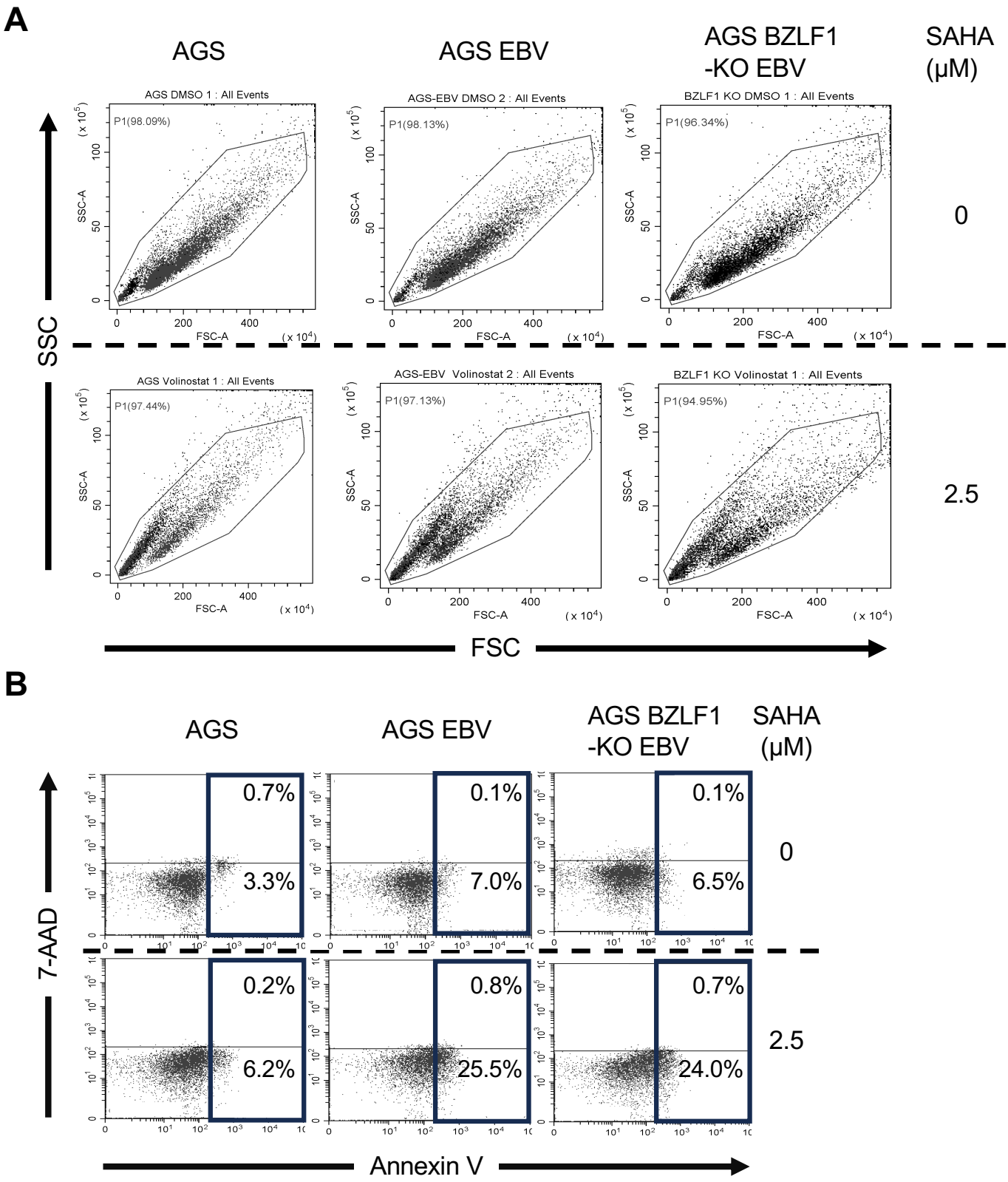

Supplementary 2

A. Two dimensional forward and side distributions of cells treated with 0 or 2.5 μM of SAHA by the flow cytometric analysis. The cells sequesterd by the black line were applied for the apoptosis assay. **B**. Histogram data of the apoptosis assay. Vertical axis: 7-AAD; horizontal axis: annexin V. Cells in early apoptosis: 7-AAD$^-$/annexin V$^+$; late apoptosis: 7-AAD$^+$/annexin V$^+$.

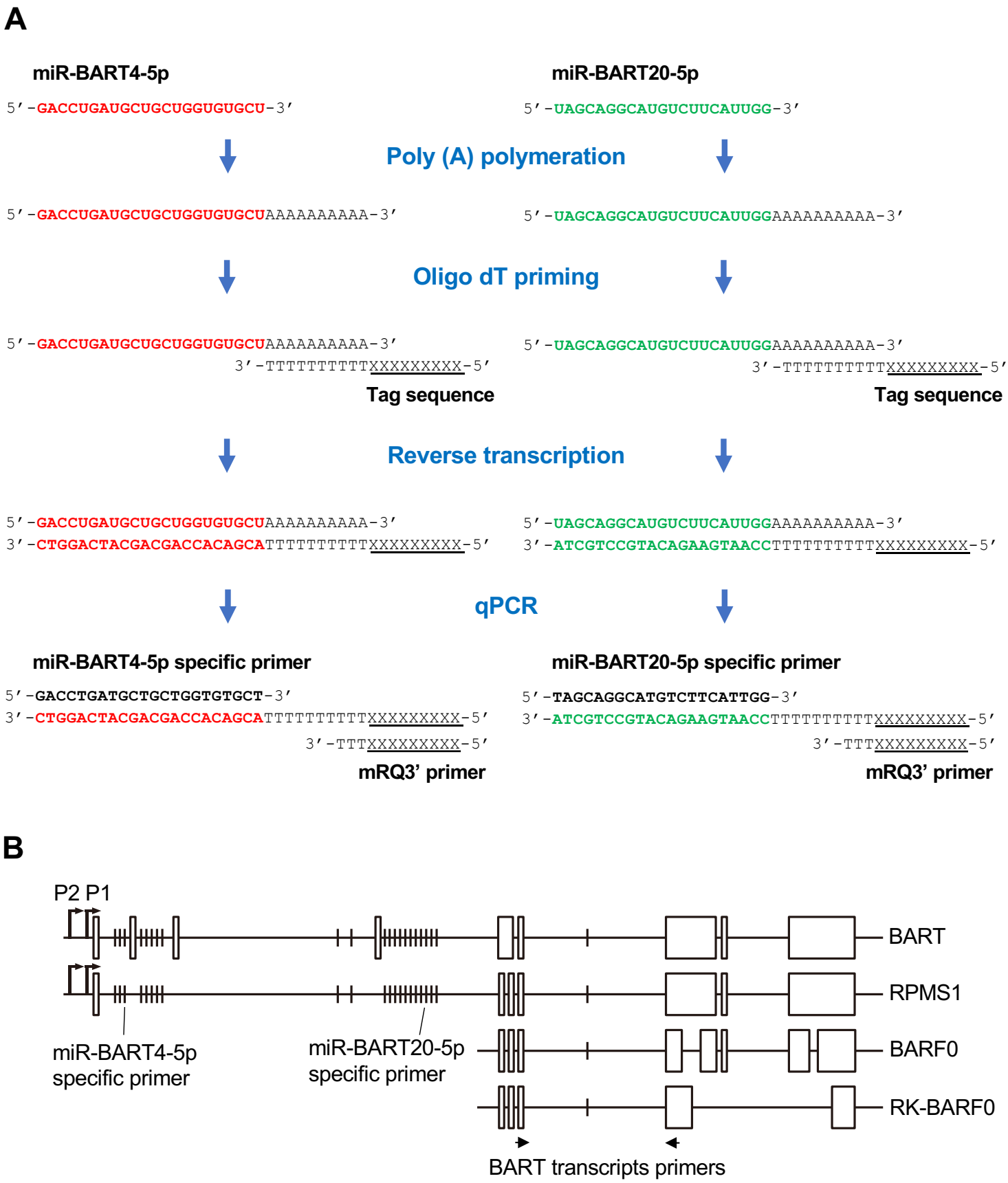

Supplementary 3

A. Procedure of the RT-qPCR assay for viral miRNAs. Red: miR-BART4-5p, Green: miR-BART20-5p. **B**. Genetic structure of BART transcripts. Arrow: BART transcripts primers.

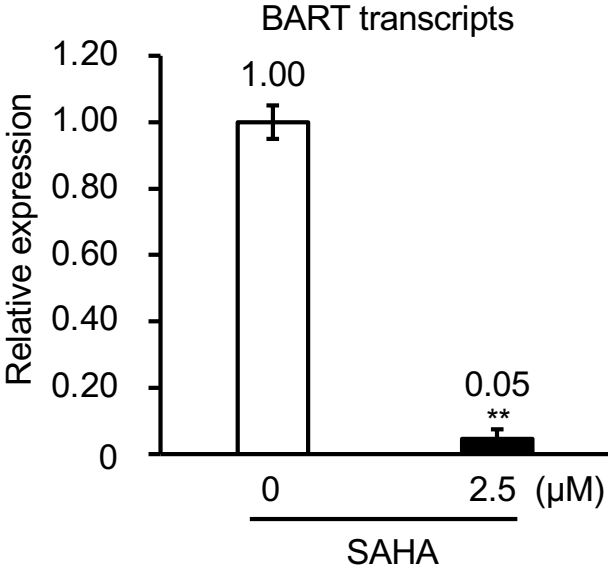

Supplementary 4

Expression of BART transcripts in SAHA-treated and untreated MKN28 EBV cells. **: $p < 0.01$.

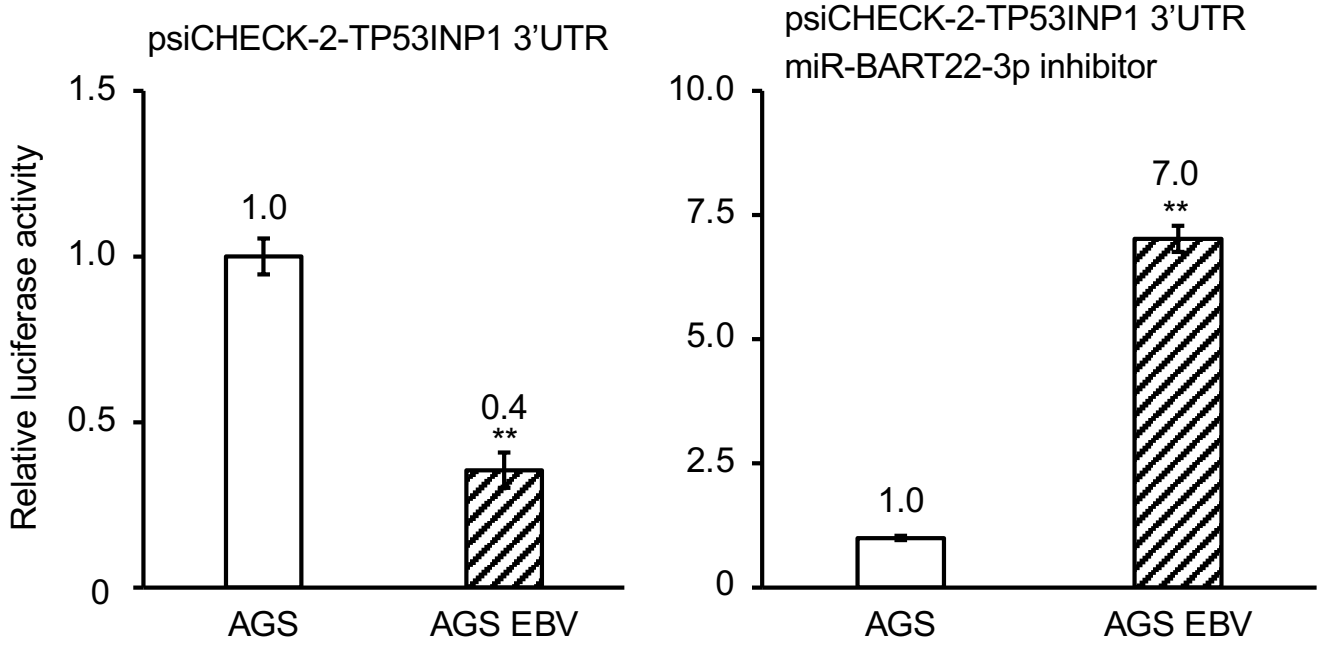

Supplementary 5

A miRNA reporter assay to measure the viral miR-BART22-3p activity. The psiCHECK-2-TP53INP1 3'UTR vector was introduced AGS or AGS EBV cells with or without miR-BART22-3p inhibitor. Both Renilla and firefly luciferase activity were measured and normalized relative luciferase activities were calculated. All results were obtained from three different samples. The expression level of AGS cells was set to 1.0 . **: $p < 0.01$.

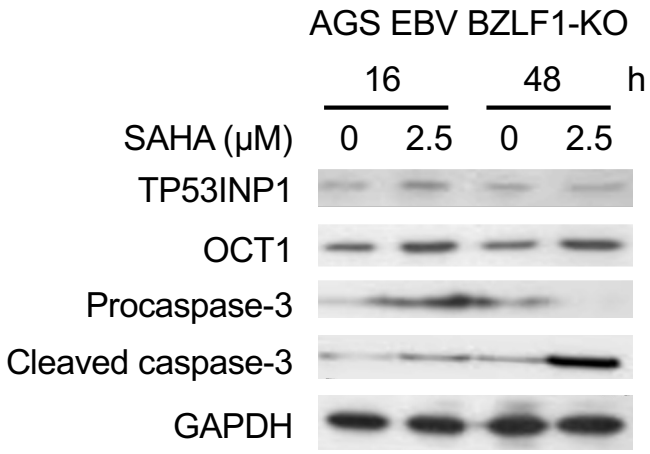

Supplementary 6

Expressions of apoptosis inducing factors in SAHA treated AGS EBV BZLF1 KO cells detected through Western blotting.